Control of spontaneous emission in photonic crystals

Misha Boroditsky[a], Rutger Vrijen[a], Thomas Krauss [b], Roberto Coccioli[a], Raj Bhat[c], Eli Yablonovitch[a]

[a] Electrical Engineering Department, UCLA
[b] Electrical Engineering Department, Glasgow University
[c] Corning

ABSTRACT

We studied enhancement and suppression of spontaneous emission in thin-film InGaAs/InP photonic crystal at room temperature. Angular resolved photoluminescence measurements were used to determine experimentally the band structure of conduction band of such a photonic crystal and overall enhancement of spontaneous emission. We demonstrated spontaneous emission enhancement in thin slab photonic crystals. It was shown that emission into the leaky conduction bands of the crystal has the same effect as cavity-enhanced spontaneous emission provided these bands are flat enough relative to the emission band of the material.

Keywords: Photonic crystals, Purcell effect, resonant enhancement, spontaneous emission.

1. INTRODUCTION

For a long time the spontaneous emission rates were believed to be an intrinsic property of a material. It was later understood that spontaneous emission also depends strongly on the surrounding environment through the density of states and local strength of the electromagnetic modes[1]. The first work on enhancement and suppression of spontaneous emission in the microwave regime were performed in 1980's by Haroche and Kleppner[2]. It was predicted by Purcell[3] that an atom in a
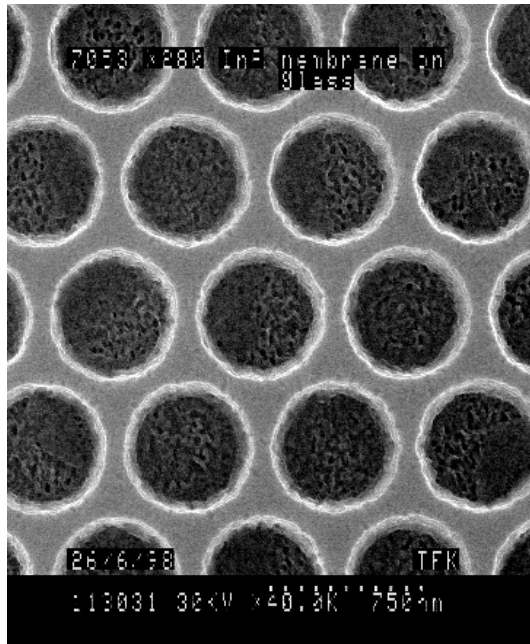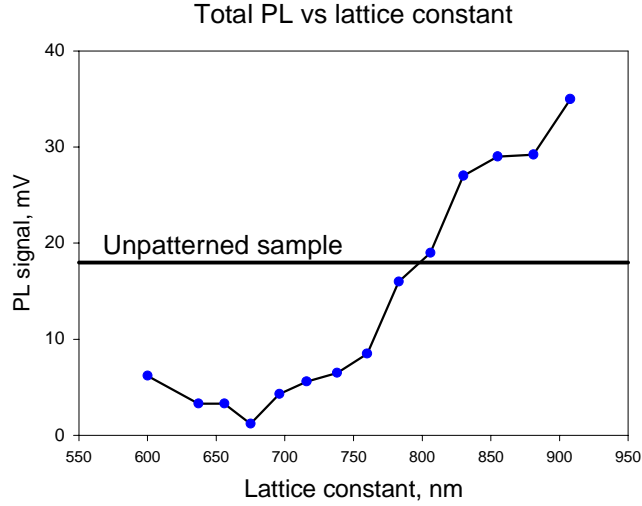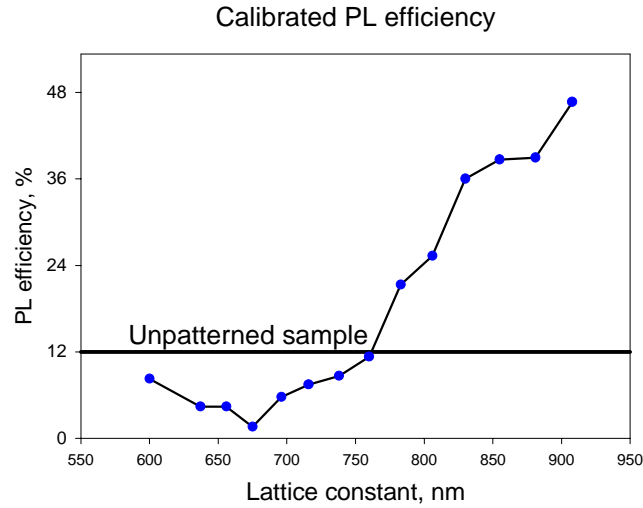

Figure 1. A triangular array of holes in the thin film on InGaAs/InP double hetero-structure. The spongy gray substance inside the holes is the optical glue. Lattice spacing is 720nm, film thickness is 240nm and hole diameter is 550nm.

wavelength-size cavity can radiate much faster than in the free space. This effect was measured in a cavity formed by two parallel mirrors by Haroche *et al.*[4]. All these measurements were performed on single atoms. A similar effect can be observed in semiconductor materials, even though the smallest chunk of the semiconductor we can imagine consists of thousands of atoms. Enhancement of the spontaneous emission rate was recently observed at low temperatures in Vertical Cavity Surface Emitting Laser type structures of small lateral dimensions[5].

Photonic crystals, artificially created, multi-dimensionally periodic structures are known for a forbidden electromagnetic bandgap. For that reason, they can be used to modify spontaneous emission. Initially, it was proposed to use photonic crystals to inhibit spontaneous emission[6], but they can be employed to enhance it as well.

Enhancement and suppression of spontaneous emission in thin film photonic crystals at room temperature is the subject of this paper.

We used angular resolved photoluminescence (PL) measurements to experimentally measure the band structure of the conduction band of such a photonic crystal and the overall enhancement of spontaneous emission. It will be shown below that emission into the leaky conduction bands of the crystal can be enhanced just like emission into a c cavity mode provided these bands are flat enough relative to the emission band of the material.

An MOCVD-grown $In_{0.47}Ga_{0.53}As$/InP single quantum well

Total PL vs lattice constant

(a)

Calibrated PL efficiency

(b)

Figure 2. (a)Photoluminescence from a thin slab photonic crystal with a triangular lattice (raw data). Thickness of the photonic crystal is t=240nm. b) the same with efficiency calibrated to the reference sample

double hetero-structure (see Table 1) was used for these experiments.

InP top cladding layer	90nm
$In_{0.47}Ga_{0.53}As$, $n=10^{18}cm^{-3}$, active region	60nm
InP bottom cladding layer	90nm
Glass slide	

Table 1. Sample structure.

Thin films for the photoluminescence experiments were fabricated using a substrate removal technique and bonded to a glass slide. A set of photonic crystal structures were etched into the thin film samples using electron-beam lithography and ion beam etching. Each sample had numerous triangular lattice structures spanning a lattice constant range sufficient for the spontaneous emission band to overlap with both the photonic bandgap and with conduction band modes. In our case of emission wavelength centered at $\lambda=1650$nm, the photonic crystal's lattice constant was made to vary from a=550nm to a=910nm. Correspondingly, the center of the photonic band gap varied from $\lambda=1300$nm to $\lambda=1900$nm (all wavelength λ are

vacuum wavelength). An SEM picture of a typical structure with a=720nm and r/a=0.37, where *r* is the radius of the holes, is shown in Figure 1.

2. ANGLE INTEGRATED PHOTOLUMINESCENCE MEASUREMENTS

All examples of a thin slab photonic crystal were measured using a standard PL setup with a 780nm AlGaAs pump laser. This gave a quick way of estimating overall photoluminescence efficiency.. The results of measurements for these lattices are shown in Figure 2. As one can see from Figure 2, the photoluminescence efficiency increases with lattice constant. The pumping conditions were fixed and the results did not depend on orientation of the pumping beam with respect to the samples. The dependence in Figure 2 represents exactly the behavior one would expect for emission into leaking conduction band modes[8]. Indeed, at small lattice constant, the semiconductor emission falls into the forbidden TE gap of the photonic crystal. The light is emitted into the TM guided modes and lost. When the spontaneous emission band overlaps with the forbidden TE gap for guided modes, emission rate is small. However, as the lattice constant of a photonic crystal becomes larger, the frequency of the photonic bandgap slides down and the emission band starts to overlap with leaking conduction band modes. Most of the photons are emitted into these guided modes of the crystal and then leak into the free space. The behavior of such photonic crystals was predicted by S.Fan *et al.*[7] for larger lattice constants but the influence of non-radiative recombination, a factor crucial for the analyses at small lattice constants, was not taken into account in their work.

3. BAND STRUCTURE MEASUREMENTS ON PHOTONIC CRYSTALS.

The angular resolved emission allows for measurements of the dispersion diagram of a photonic crystal's leaky modes, that is modes with frequencies lying above the light cone in glass. Indeed, as discussed above, any eigenmode of a thin slab photonic crystal with the in-plane wave vector $\mathbf{k}_\parallel$ must satisfy Bloch condition for in-plane propagation

$$\mathbf{E}(\mathbf{r},t) = \mathbf{U}(\mathbf{r},t)e^{-i\mathbf{k}_\parallel \cdot \mathbf{R}} , \qquad (1)$$

where $\mathbf{U}(\mathbf{r})$ has the periodicity of a crystal. On the other hand, the wave function of the mode outside of the slab, in the air or in the glass must be a plane wave asymptotically.

$$\mathbf{E}(\mathbf{r},t) \sim e^{-i(\mathbf{k}_\parallel \cdot \mathbf{R} + \mathbf{k}_\perp \cdot \mathbf{R})} , \qquad (2)$$

where $\mathbf{k}_\perp$ is the out-of-plane component of the wavevector, so that the propagation angle is $\alpha = \arctan(\mathbf{k}_\parallel / \mathbf{k}_\perp)$. Then, keeping in mind that for the modes above the line light $\omega(\mathbf{k}_\parallel) > \mathbf{k}_\parallel c / n$, we conclude that relation

$$\left(\frac{\omega(\mathbf{k}_\parallel)n}{c}\right)^2 > \mathbf{k}_\parallel^2 + \mathbf{k}_\perp^2 \qquad (3)$$

can not be satisfied for real ω and **k**. Thus the modes in the region above the light line have to be leaking and hence detectable. From the information on frequency versus emission angle we are able to reconstruct the band structure of the leaking modes. We used the spontaneous emission spectral peaks versus angle to study the bandstructure of the photonic crystal. A typical sequence of spectra corresponding to the various angles of is shown in Figure 3 for 29, 32 and 35 degrees. A smooth evolution of the peaks is clearly visible. Our spectral data in Figure 4 showed also, that, even though the modes of a thin film photonic crystal can not be classified as pure TE or pure TM, some of them have strongly dominating TE or TM components, while others are more mixed. If so, the photoluminescence at large angles must be polarized depending on the dominant polarization of a corresponding leaky mode. We used a polarizing beam-splitter to select the different polarizations. As can be seen from the Figure 4, the broad background turned out to consist of a few clearly polarized (or
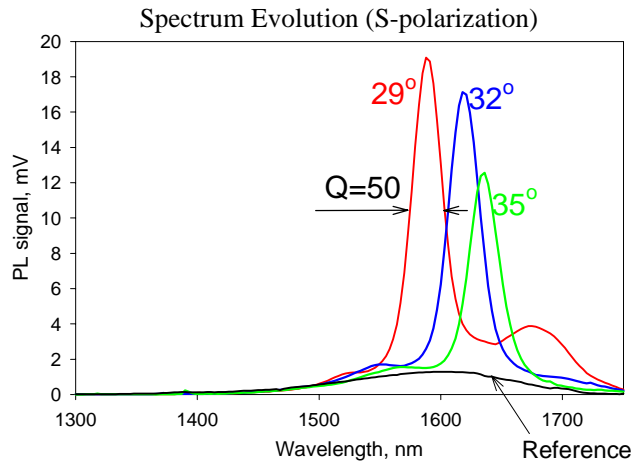
Figure 3. Measured angular resolved emission with respect to the normal axis spectra have relatively high Q between 30 and 100 and peak to background ratio about 15.
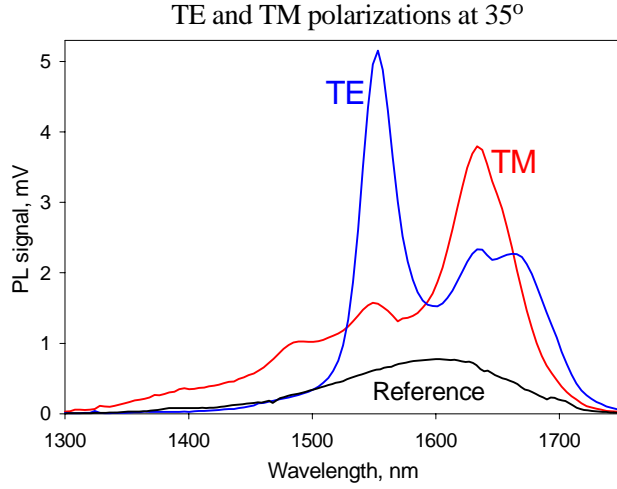
TE and TM polarizations at 35°

Figure 4. Some modes are well polarized while others are of mixed polarization.

sometimes mixed) peaks.

Plotting values of the spectral peak positions versus angle allows us to re-plot the graph (see Figure 5) on the frequency versus in-plane $k_{//}$ using expressions derived earlier in the section. All detectable bands above the light line correspond to leaky modes, and that permits us to measure them. The recorded spectrum of the photoluminescence consists of peaks corresponding to the leaky modes and a broad bell-shaped background corresponding to the emission into the 3D continuum of extended modes. The coupling overlap of the leaky modes with the active region of the photonic crystal is determined by the internal structure of the mode. The farther the mode is from the light line the easier it is to detect. Also, some of the conduction band modes of the photonic crystal have their electric field concentrated in the air regions. Thus, electron-hole pairs can not emit efficiently into these modes and it is difficult to observe them.

Comparing the measured band structure in Figure 5 with the overlaid dispersion diagram computed using the Finite Difference in Time Domain technique[8], we see a good agreement in the shape of the curves as well as in their polarization. A triangle formed by the crossing of the lowest TE and TM conduction bands in Figure 5 is a typical and repeatable feature in several samples with different lattice constants. This is the first, to our knowledge, demonstration of spontaneous emission directly into the photonic bands and the first measurement thereof. Angular resolved spectra on thin film photonic crystals reveal some very sharp peaks (compared to the emission linewidth of InGaAs), with a Q between 100 and 30, a feature that was not present in previous experiments on thicker films. Besides the high Q, another important feature of the figure is a very high peak to background ratio, around 15, as can be seen from Figure 3. In the following section we will argue that these are signatures of the Purcell enhancement realized without a cavity.

4. RESONANT ENHANCEMENT IN THIN-SLAB PHOTONIC CRYSTALS

It was shown[9] that spontaneous emission in a small cavity is faster than in the bulk material. Crucial parameters for the speedup were cavity Q and effective volume V_{eff} of the resonant mode:

$$\frac{\Gamma}{\Gamma_0} = \frac{3Q_m g(\lambda/2n)^3}{2\pi V_{eff}}$$

(4)

In the photonic crystals studied in the previous section, the measured Q's of modes were comparable to that of a dielectric cavity. Since these modes are large in volume, local field enhancement is much smaller. But since the band structure of upper modes is nearly flat as can be seen from both theoretical and experimental results (Figure 5), these modes pick up a large degeneracy factor, g, compensating the loss in the local field enhancement.

Now we will derive the enhancement of spontaneous emission in a particular direction:

Suppose we have selected a narrow solid angle $\sin\theta d\theta d\phi$ and a frequency range $d\omega$. Then, similarly to the derivation in Ref 9, we have to compare the density of modes and local fields of the emission into a 3-d continuum of modes to that of the emission into the leaky guided modes.

The spontaneous emission rate is proportional to square of the local field of the mode $E^2(\mathbf{r})$ (normalized to $h\nu/2$) and to the number of modes ΔN emitting into the given solid angle in given frequency range.
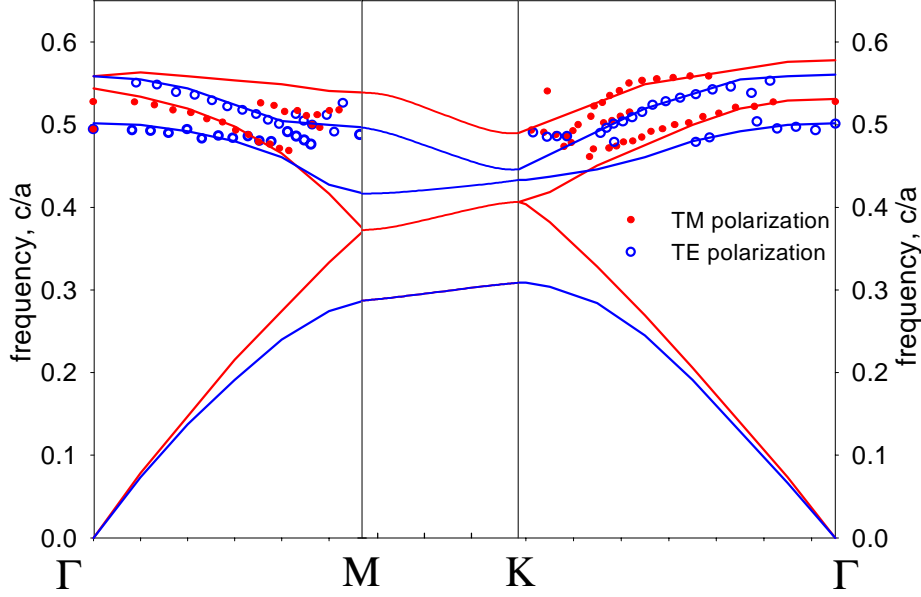
Figure 5. Theoretical and experimental bands for the photonic crystal from Figure 1. Red lines correspond to TM-like modes, blue lines are TE like modes.

For emission into the 3-d continuum of modes,

$$\mathbf{E}^2(\mathbf{r}) = \frac{\hbar\omega}{2nV} \ , \tag{5}$$

And number of modes emitting into the given solid angle is given by

$$\Delta N_{3d} = 2\frac{k^2 \sin\theta\, dk\, d\theta\, d\phi}{(2\pi)^3} V \ , \tag{6}$$

where k=ω/c is a corresponding wavevector and V=L^3 is the quantization volume.

For the case of emission into the leaky modes, the local field depends on the position of the emission dipole in the active region. We can assume that vertical distribution of the electric field is concentrated in a slab waveguide. Then, the average square of the electric field normalized by a single quantum in a given point is given by

$$\mathbf{E}^2(\mathbf{r}) = \frac{\hbar\omega}{2\int_{slab}\varepsilon(\mathbf{r}')\mathbf{E}_0^2(\mathbf{r}')d^3\mathbf{r}'}\mathbf{E}_0^2(\mathbf{r}) \approx \frac{\hbar\omega}{2(t/2)\int_{slab}\varepsilon(\mathbf{r}')\mathbf{E}_0^2(\mathbf{r}')d^2\mathbf{r}'}\mathbf{E}_0^2(\mathbf{r}) \ , \tag{7}$$

where t is the slab's effective thickness and $\mathbf{E}_0$ is the non-normalized electric field distribution of the mode. Integration in the last expression is performed over the center plane of the slab.

The number of modes emitting at this angle is given by a projection of the three-dimensional k-space onto the plane of guided mode wave vectors:

$$\Delta N_{3d} = 2\frac{k_\| dk_\| d\phi}{(2\pi)^2} A \ , \tag{8}$$

where $k_{//}=k\sin\theta$, $dk_{//}=k\cos\theta d\theta$ and A=L^2 is the area of the slab.

Averaging over the active region A_{active} in a unit cell would give the total radiation rate in a given direction. However, since the line width of the leaky mode $\Delta\omega$ is much larger than specified spectral resolution dω, only $\frac{2}{\pi}\frac{d\omega}{\Delta\omega}$ of the radiation will be in the spectral range. The 2/π pre-factor comes from the Lorentzian lineshape of the leaky mode, similar to the derivation in Chapter 3.

Thus, the rate of background radiation would be given by

$$\Gamma_{3d} \propto \int_{active} \mathbf{E}^2(\mathbf{r})\Delta N_{3d}d^2r = 2\frac{k^2\sin\theta dkd\theta d\phi}{(2\pi)^3}V\cdot\frac{\hbar\omega}{2nV}\cdot A_{active} \tag{9}$$

And, in the same way, emission into the leaky modes is

$$\Gamma_{2d} \propto \int_{active} \mathbf{E}^2(\mathbf{r})\Delta N_{2d}d^2r = \frac{\hbar\omega}{2(t/2)\int_{slab}\varepsilon(\mathbf{r'})\mathbf{E}_0^2(\mathbf{r'})d^2\mathbf{r'}}\cdot\frac{2d\omega}{\pi\Delta\omega}\frac{(k\sin\theta)(k\cos\theta d\theta)d\phi}{(2\pi)^2}\int_{active}A\mathbf{E}_0^2(\mathbf{r})d^2r \tag{10}$$

Taking a ratio and simplifying we get:

$$\frac{\Gamma_{2d}}{\Gamma_{3d}} = \frac{1}{\pi}\frac{A_{slab}}{\int_{slab}\varepsilon(\mathbf{r'})\mathbf{E}_0^2(\mathbf{r'})d^2\mathbf{r'}}\cdot\frac{\int_{active}\varepsilon\mathbf{E}_0^2(\mathbf{r})d^2r}{A_{active}}\cdot\frac{\omega}{\Delta\omega}\frac{\lambda}{nt}\cos\theta \tag{11}$$

Introducing mode's $Q=\omega/\Delta\omega$, and a parameter γ to characterize electric energy overlap with the active region:

$$\gamma = \frac{A_{slab}}{\int_{slab}\varepsilon(\mathbf{r'})\mathbf{E}_0^2(\mathbf{r'})d^2\mathbf{r'}}\cdot\frac{\int_{active}\varepsilon\mathbf{E}_0^2(\mathbf{r})d^2\mathbf{r}}{A_{active}} \tag{12}$$

enhancement of spontaneous emission rate at a given frequency can be transformed into a familiar structure of a Purcell number in 1 dimension:

$$\frac{\Gamma_{2d}(\omega)}{\Gamma_{3d}} = \frac{2\gamma}{\pi}Q\cdot\frac{\lambda}{2nt}\cos\theta \tag{13}$$

In semiconductors, the emission band is normally wider than the cavity linewidth. For that reason the Lorentzian in Equation (13) has to be convoluted with the semiconductor emission spectrum, as it is done in derivation of Purcell factor. This integrates out the $2/\pi$ in the Lorentzian and substitutes Q with the material's Q_m (10 for InGaAs in our case). Then the spectrally integrated enhancement in a given direction becomes

$$\frac{\Gamma_{2d}}{\Gamma_{3d}} = \gamma Q_m\cdot\frac{\lambda}{2nt}\cos\theta \tag{14}$$

In the structure we have studied, the active region covers approximately half of the sample area. In the optimal case, when all electric energy of the mode is concentrated in the semiconductor, the overlap parameter is simply $\gamma\approx 2$. This happens close to the Γ point of the Brillouin zone, as can be seen from the computed energy distribution plot in Figure 6. Then, expected peak enhancement, i.e the peak to background ratio of the spectra in Figure 2, in a direction close to the normal would be $\frac{\Gamma_{2d}}{\Gamma_{3d}} \le 2\cdot\frac{2}{\pi}Q\cdot\frac{1650}{7\cdot 240}\approx Q$, i.e. approximately the modal Q. The observed peak to background ratio is smaller, about 15 to

20. We attribute this discrepancy to two factors: First, the background may be higher due to the contribution of other modal peaks, and, second, the structure imperfections may cause some additional scattering of the mode.
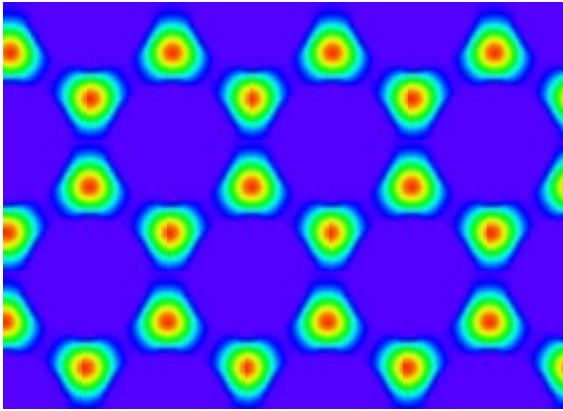

Figure 6. Electric energy distribution in the Γ point of the Brillouin zone. All energy is concentrated in the dielectric veins.

If the photonic bands could be engineered to be relatively flat compared to the emission spectrum, this enhancement would be achieved for all directions. As can be seen from the experimental and theoretical band structures of the photonic crystal that we considered, the spectral variation of the lowest "conduction" band is approximately twice the spontaneous emission band. Then, the enhancement integrated over all the angles becomes somewhat smaller, between 3 and 5. If the band can be made flat, the radiative lifetime can be made influenced by Purcell effect.

In the best of the thin slab photonic crystals, the photoluminescence efficiency was considerably greater than in unpatterned samples. Absolute efficiency calibration can be made by referencing the emission to the reflection (100%) froom a white surface. Such calibration generally shows that InGaAs double hetero-structures grown by Raj Bhat, have an internal quantum efficiency near 100%.
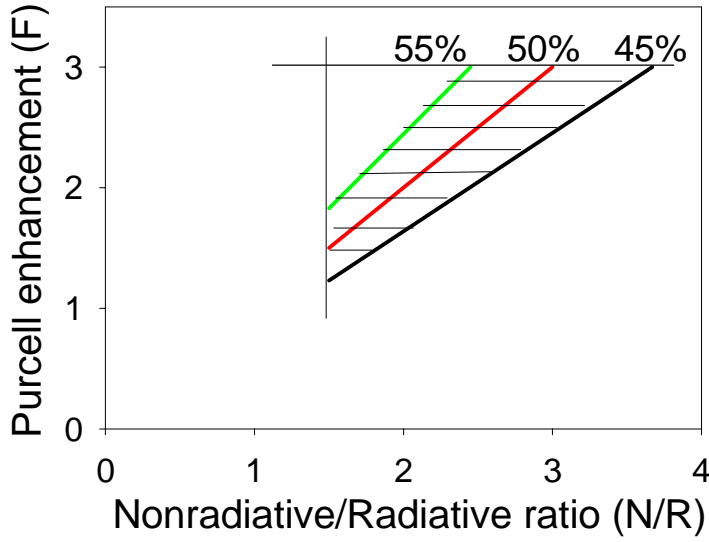
Figure 7. Dependence of the Purcell enhancement factor on the value of the non-radiative recombination rate N/R for different values external efficinecy η=45, 50, 55%. The shaded area limits the possible values of the Purcell enhancement factor. The Purcell factor is constrained by the lower limit on N/R=1.5 from the left, and by the maximum Purcell factor 3 in this kind of structure from the top.

An unpatterned thin film between two glass hemispheres has an optical escape probability of $2\dfrac{1}{4(n_f/n_g)^2} \sim 0.11$, where n_f=3.2 and n_g=1.5 are refractive indices of the semiconductor film and glass correspondingly. In our ultra-thin films, the effective refractive index is probably slightly smaller than that of the bulk material. Also, the high internal efficiency of the InGaAs active layer allows the photon recycling to boost the external efficiency of the film even higher. With all these benefits combined, we conservatively estimate that a thin film, when encapsulated in glass or epoxy, can have a double sided 12% external efficiency. This sets an absolute efficiency scale for the photonic crystal samples shown in the Figure 2b, (which were all measured under identical pump and collection conditions). The calibrated photoluminescence signal versus lattice spacing is shown in Figure 2a. As can be seen from the graph, the PL strength from the photonic crystal samples with lattice constant ~900nm, where conduction band modes match the InGaAs emission frequency, is twice as large as that from an unpatterned sample. Taking into account that there is only half as much surface area in the patterned PBG samples to absorb light (at least in the geometrical optics approximation), this gives the external efficiency of 4×12=48%. There are three factors influencing the measured external quantum efficiency of photonic crystal samples:

1. In principle, the extraction efficiency can be unity since all modes are leaky.

2. By drilling the holes through the active region, we introduce non-radiative recombination. We will show below that non-radiative recombination rate N is comparable to the radiative emission rate R: $N/R\sim1$, where R is the radiative emission rate in bulk semiconductor material in which there is no Purcell effect.

3. The radiative emission rate in the patterned film is enhanced by the Purcell factor F, a quantity we would like to determine: R→FR.

Then, the external quantum efficiency of the sample emitting into the conduction band modes of the photonic crystal would be given by the fractional rates:

$$\eta = \frac{FR}{FR+N} = \frac{F}{F+N/R},\qquad (15)$$

which can be solved for the Purcell enhancement factor F:

$$F = \frac{\eta}{1-\eta}\cdot\frac{N}{R}\qquad (16)$$

It follows from the Equation (16) that the knowledge of relative non-radiative recombination rate (N/R) is necessary to determine the Purcell factor.

We can use the a=600-700nm samples in Figure 2b emitting into the forbidden photonic bandgap to estimate the non-radiative recombination rate. Indeed, as can be seen from the Figure 2b, the total photoluminescence signal in those samples is 5 times lower than in the unpatterned sample. Correcting for pumped area ratio, a factor of 2 as before, gives us a 2.5 times drop in the external efficiency compared to the unpatterned continuous film, as shown if Fig 2a. Using a conservative assumption that the escape probability is the same as in unpatterned film, we obtain an estimate on non-radiative recombination rate N in terms of the radiation recombination rate R:

$$\frac{R}{R+N} < 0.4\qquad (17)$$

from which follows N/R>1.5.

The factor 1.5 is a lower limit on the non-radiative/radiative recombination rate because the extraction efficiency of the sample with holes is more likely to increase due to the presence of additional surfaces. Plotted in Figure 7, is a family of curves showing the dependence of Purcell enhancement factor versus (N/R) for different efficiencies from Eqn. (16). As one can see from the Figure 7, the Purcell factor is constrained by our measurements to be above 1.5 but probably less than the F=3 which would occur in the ideal case at room temperature in InGaAs. Certainly, we will need to perform lifetime measurements on our samples to verify the exact value of the Purcell factor for spontaneous emission into conduction band modes.

5. SUMMARY

The results of photoluminescence measurements on thin slab photonic crystals were presented in this paper. The angle dependence of the PL spectral peaks was shown to follow the photonic bands of the photonic crystals. The band structure of the conduction bands was measured using the angular resolved spectra. Up to a 15-fold enhancement of the emission in a given direction was observed and explained in terms of the Purcell enhancement.

REFERENCES

1. P. Selenyi, Phys. Rev. **56**, 477-480 (1939)
2. R.G.Hulet, E.S. Hilfer, D. Kleppner, Phys. Rev. Lett, **59**, 2955 (1955)
3. E.M. Purcell, Phys. Rev. **69**, 681(1946)
4. P. Goy, J.M. Raimond, M. Gross, S. Haroche, Phys. Rev. Lett. **50,** 1903 (1983)
5. J. Gérard, B. Sermage, B. Gayral, B. Legrand, E. Costard, V. Tierry-Mieg, "Enhanced spontaneous emission by quantum boxes in a monolithic optical microcavity, "*Phys. Rev. Lett.*, 1998, 91(5), pp. 1110-1113.
6. E. Yablonovitch, 'Inhibited spontaneous emission in solid-state physics and electronics,' *Phys. Rev. Lett.*,1987, **58** (20), pp. 2059-2062.
7. S. Fan, P. Villeneuve, J. Joannopoulos, E.F. Schubert, Phys. Rev. Lett. **78**, 3295, (1997)
8. M. Boroditsky, R. Coccioli, E. Yablonovitch, "Analysis of photonic crystals for light-emitting diodes using the finite difference time domain technique", Proc. Photonics West '98, San Jose, CA, 26-30 Jan. 1998, vol. **3283**, p.184-90.
9. R. Coccioli, M. Boroditsky, K. Kim, Y. Rahmat-Samii, E. Yablonovitch, "What is the Smallest Possible Electromagnetic Mode Volume in a Dielectric Cavity?" to be published in IEE Proceedings – Optoelectronics.